



Cite this: *Phys. Chem. Chem. Phys.*,
2014, 16, 22958

Received 5th September 2014,
Accepted 10th September 2014

DOI: 10.1039/c4cp03984j

www.rsc.org/pccp

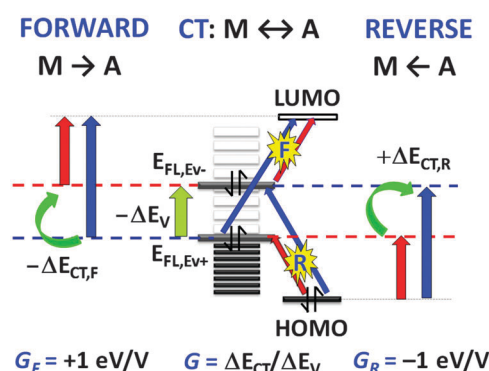
On the dual character of charged metal–molecule hybrids and the opposite behaviour of the forward and reverse CT processes†

J. Roman-Perez, S. P. Centeno, M. R. López-Ramírez, J. F. Arenas, J. Soto,
I. López-Tocón* and J. C. Otero*

DFT calculations predict two different electronic structures of metal–molecule hybrids which are selected depending on the surface charge. While the metal-to-molecule CT states are very sensitive to the charge, the energies of the reverse molecule-to-metal CT processes are surprisingly not modified at all by the charge of the metal.

Charge transfer (CT) in metal–adsorbate (M–A) hybrids is a key process involved in many technological devices.^{1,2} In spite of the large number of studies dealing with this simple process some basic questions are still not well understood. This is the case of the unexpected efficiency of the electrode potential (E_V) in tuning the energy of the forward metal-to-molecule CT states (E_{CT}) observed, for instance, in surface-enhanced Raman scattering (SERS).^{3,4} Huge energy gains ($G = \Delta E_{CT}/\Delta E_V$) of up to 5 eV V^{-1} have been reported from electrochemical SERS experiments. This cannot be understood from a classical view of the CT process (Scheme 1 and S1, ESI†), given that the energy of the forward or reverse (F/R) metal–molecule CT-processes would be red or blue-shifted ($\Delta E_{CTF}/\Delta E_{CTR}$) by as much as -1 or $+1 \text{ eV}$, respectively, when the electrode potential shifts by -1 V ($-\Delta E_V$).⁵ The main shortcoming of the very popular CT models analogous to that presented in Scheme 1 is that both metal and adsorbate are considered to be non-interacting subsystems, which is implied by the equivalence between the slopes in Scheme S1b and c (ESI†) ($G_F = -G_R = 1 \text{ eV V}^{-1}$) irrespective of the nature of M and A.

This conclusion contradicts the experimental values of G which are very sensitive to the nature of the complex as well as to other experimental variables. Recently, we demonstrated⁶ that two contributions are involved in the energy gain $G = SC = E_{CT}/E_V$. C is a kind of electrical capacitance that quantifies the capability of the metal to convert the applied macroscopic electrode potential for changing the charge of the surface metal



Scheme 1 Standard energy diagram to visualize metal–molecule M–A CT processes between the Fermi level of the metal and the occupied (HOMO) or vacant (LUMO) orbitals of the adsorbate, showing the effect of a negative shift of the electrode potential ($-\Delta E_V$) on the Fermi level ($E_{FL,Ev+} \rightarrow E_{FL,Ev-}$). This results in a red shift of the forward (F) metal-to-molecule CT_F energy ($E_{FL}(M) \rightarrow LUMO(A)$) or a blue shift of the reverse (R) molecule-to-metal CT_R energy ($HOMO(A) \rightarrow E_{FL}(M)$). From these widely used schemes, an equivalence between both energy quantities ($\Delta E_{CT} = e\Delta E_V$) is deduced giving trivial energy gains of $G = \pm 1 \text{ eV V}^{-1}$, respectively. This is in disagreement with both the experimental results for CT_F ($G_F \gg 1 \text{ eV V}^{-1}$) and the prediction made in this communication for the reverse CT_R process when the negatively charged isonicotinate is involved ($G_R \approx 0 \text{ eV V}^{-1}$).

atom to which the molecule is adsorbed ($C = q/E_V$). In turn, S quantifies the dependence of the energy of the CT states of the hybrid system on the atomic surface charge ($S = E_{CT}/q$). As we shall show, S is the most subtle and unforeseeable contribution as it depends on a particular state, the nature of the metal and the molecule and on the experimental conditions too. Widely used CT diagrams like those shown in Scheme 1 and S1 (ESI†) are absolutely incompatible with some experimental evidence and the predictions derived from the present work. As shown in these diagrams, the Fermi level of the metal ($E_{FL,Ev}$) is raised up to $+1 \text{ eV}$ when a negative shift of -1 V is applied to the electrode potential. Moreover, the CT_F or CT_R processes originate due to the transfer of a complete electron between the Fermi level of the metal ($E_{FL,Ev}$) and vacant (LUMO) or occupied (HOMO) molecular

Universidad de Málaga, Facultad de Ciencias, Dept. de Química Física,
Unidad Asociada CSIC, 29071-Málaga, España. E-mail: tocon@uma.es,
jc_otero@uma.es; Fax: +34 952132019; Tel: +34 952132019

† Electronic supplementary information (ESI) available: Computational details and tables and figures mentioned in the text. See DOI: 10.1039/c4cp03984j

orbitals of the adsorbate, respectively. Scheme 1 cannot explain how $\Delta E_V = 1$ V can be amplified up to $\Delta E_{CT,F} = 4$ eV,⁶ but it seems even more difficult to explain how the reverse mechanism could be insensitive to the electrode potential. Providing explanation for these discrepancies is the objective of this work.

Many CT processes take place in true M–A complexes where M and A are chemically bonded and cannot be considered as separate moieties. In these cases, CT occurs between the ground electronic state of the hybrid and excited states with a CT character. The electrode potential just modifies the surface excess of charge of the metal and this process is controlled through the electrical capacitance C . Each surface charge generates a new M–A chemical species and modifies all the electronic structures of the particular hybrid in an unknown, either large or small, extension. This affects the properties of the ground electronic state, like the M–A bond energy, and especially those of the CT excited states. This subtle mechanism is controlled by the slope S .

At present, the only operative way to get insight into the complex CT mechanism in true M–A hybrids is to resort to electronic structure calculations. In two previous communications^{7,8} we have introduced a methodology to study theoretically the relationship between the charge of the metal and the electronic structure of the surface complex, *i.e.*, the energy of the CT states. It is based on time-dependent (TD) DFT calculations carried out on the ground and excited states of complexes formed by a molecule bonded to linear stick-like metal clusters $(M_n)^q$ of different sizes ($n = 2, 3, 5$ and 7) and charges ($q = 0, \pm 1$ a.u.), giving the corresponding metal–adsorbate $[(M_n)^q\text{--}A]$ systems (Fig. 1a, bottom). These $(M_n)^q$ clusters allow us to account smoothly for the effect of a fractionary charge excess on the electronic structure of the M–A complex. In all the ground and excited electronic states some amount of charge is interchanged between M and A, but true

CT states are easily recognized by comparing the corresponding Mulliken's net charges of the Ag_n clusters (or the adsorbate) in the ground S_0 and the corresponding singlet excited state S_1 . More complex redistribution of charges between M and A, like back-donation, are not discussed here. Theoretical calculations have been carried out by using the Gaussian 09 suite of programs⁹ and are detailed in the ESI,[†] where a complete set of selected results concerning the ground S_0 and the CT states have been summarized. The mentioned previous studies^{6–8} were focused on the excited CT states whose energies are linearly dependent on $q_{\text{eff}} = q/n$:

$$E_{CT} = S q_{\text{eff}} + E^0 \quad (1)$$

where q_{eff} is the microscopic analogue to the macroscopic charge excess q_M' (C/cm^2 of surface) and quantifies the atomic charge excess averaged amongst the metallic atoms (a.u. per atom of surface), ranging from -0.33 to $+0.33$ for the respective Ag_3^{-1} and Ag_3^{+1} complexes. In the cases of pyridine, pyrazine and isolated or protonated adenine linked to Ag or Rh clusters, the CT process is dominated by the forward metal-to-molecule $M \rightarrow A$ electron transfer in the UV-Vis range of energies.^{6–8}

Fig. 1a shows the dependence of the TD-M06-HF¹⁰/LanL2DZ¹¹ vertical energies of selected singlet excited states of silver–pyridine complexes $[Ag_n\text{--}Py]^q$ on q_{eff} . Four series of forward metal-to-molecule CT_F states below 6 eV have been drawn.⁷ All of them show a linear dependence on q_{eff} but very different slopes. The two lowest ones, $CT_{F0}; B_1$ and $CT_{F1}; A_2$, are very sensitive ($S = 6.71$ and 7.43 eV a.u.^{−1} respectively) to q_{eff} being stabilized at around 4 eV when q_{eff} varies from $+0.33$ to -0.33 ($\Delta q_{\text{eff}} = -0.66$). For the sake of comparison, the energies of the first excited singlet of pyridine $S_{1,Py}; B_1$ are also presented. This excitation is mainly localized in the adsorbate (HOMO \rightarrow LUMO in Scheme 1), and therefore no dependence on q_{eff} should be expected, given the very small transferred charge in this case ($\Delta q_t = q_{Py,Si} - q_{Py,S0}$) which amounts to less than 10% of the corresponding $CT_{Fi=0,1}$ series. In spite of this, $S_{1,Py}$ shows an S value much larger than that of the secondary series of true $CT_{Fi=1,0'}$ states. The differentiated behaviour of the five states is quantified through the respective slopes. All of them are positive but numerically very different, ranging from $S_F = 0.39$ up to 7.43 eV a.u.^{−1} In contrast, the first series of molecule-to-metal $CT_{R0}; A_2$ states lies above 6 eV, showing a negative slope as expected for reverse processes ($S_R = -4.05$ eV a.u.^{−1}), but much smaller than that of CT_{Fi} . This complex and unexpected behaviour cannot be understood at all on the basis of the simple model presented in Scheme 1, given that S is highly dependent on the particular CT (or even non-CT) state. Fig. 1a also indicates that Py does not undergo redox processes in the ground S_0 state in the overall range of scanned $\Delta q_{\text{eff}} = 0.66$, but it can be transiently photoexcited up to a $CT_F; Ag^+-Py^-$ state at $q_{\text{eff}} = -0.15$ a.u. under 514.5 nm Vis radiation, which accounts for the selective enhancement of Raman lines due to a resonant metal-to-molecule CT_F process detected in the SERS recorded at negative electrode potentials.⁸

Fig. 1b shows the energies of the same states but referred to a common zero namely, the energy of the metallic clusters (Ag_n^q)

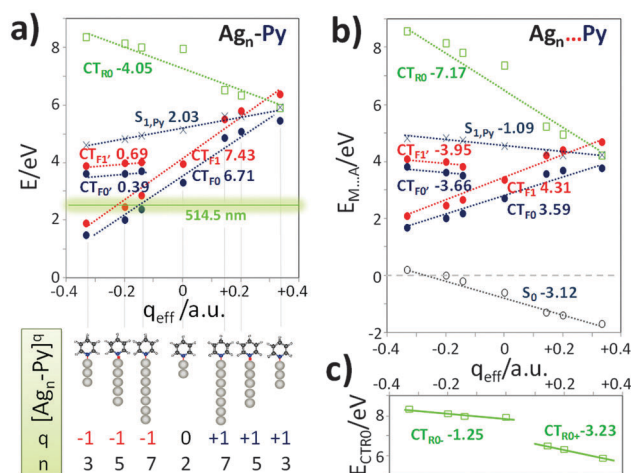


Fig. 1 (a) TD-M06-HF/LanL2DZ vertical energies (E) of the forward (CT_{F0} , CT_{F1} , $CT_{F0'}$, $CT_{F1'}$) and reverse (CT_{R0} , redrawn in (c)) charge transfer states of $[Ag_n\text{--}Py]^q$ complexes and the first excited singlet of pyridine ($S_{1,Py}$) vs. the effective charge q_{eff} . (b) TD-M06-HF/LanL2DZ energies of the same states but referred to the energy of the respective metallic clusters (Ag_n^q) and the adsorbate (Py) at infinite separation ($E_{M...A}$) (each label is accompanied by the slope S (eV a.u.^{−1}) in eqn (1)).

and the adsorbate (Py) at infinite separation ($E_{M\cdots A}$). This makes evident the stabilities (bond energy) of the respective complexes in their ground state S_0 which are also highly dependent on q_{eff} . As expected, a positive q_{eff} stabilizes the adsorption of Py on the surface through the nitrogen atom giving a perpendicular surface orientation. The M–A bond energy in S_0 amounts to -1.7 eV (-38.8 kcal mol $^{-1}$) at $q_{\text{eff}} = +0.33$, while the $[\text{Ag}_3\text{-Py}]^-$ complex should be weakly bonded. The slopes for each series of states are modified from those shown in Fig. 1a, showing either positive ($\text{CT}_{\text{Fi}=0,1}$) or negative values ($\text{CT}_{\text{Ri}=0,1}$, S_0 and $S_{1,\text{py}}$). In conclusion, q_{eff} smoothly modifies the electronic structure of Ag–Py surface complexes by tuning the energies of CT and even non-CT states in a continuous way in the range $\Delta q_{\text{eff}} = 0.66$.

A similar study has been carried out on the isonicotinate anion ($\text{in}^- = 4\text{-pyridinecarboxylate}$), a negatively charged derivative of pyridine in which the reverse molecule-to-metal CT_{R} process is expected at a much lesser energy than in the case of neutral adsorbates like pyridines. This species can be bonded to silver through nitrogen as in pyridine (Nin^-), or through the oxygen atoms of the carboxylate (Oin^-), giving the respective $[(\text{Ag}_n)^q\text{-Nin}^-]^{q-1}$ or $[(\text{Ag}_n)^q\text{-Oin}^-]^{q-1}$ complexes which have also been constrained to C_{2v} symmetry (Fig. 2c). Fig. 2a shows the first series of TD-M06-HF CT states for the most stable $[(\text{Ag}_n)^q\text{-Oin}^-]^{q-1}$ complex where a completely opposite behaviour of the forward and reverse processes can be seen. Under positive or zero q_{eff} the first two series of metal-to-molecule forward $\text{CT}_{\text{Fi}=0,1}$ states are continuously tuned as in pyridine, showing large slopes of $S_{\text{F}} = 4.90$ and 6.17 eV a.u. $^{-1}$ respectively, and therefore providing high energy gain G_{F} . Excitation up to these states results in the transient formation of the respective radical dianion of the adsorbate (Oin^{2-}), a species far less stable than that formed in the case of neutral ones like Py ($\text{Py}^{\bullet-}$). In spite of the repulsion between the two negative charges, $\text{CT}_{\text{R}0}$ is also reachable under 514.5 nm excitation at negative q_{eff} , as we observed in the SERS of the

analogous benzoate anion.¹² Forward CT_{F} states disappear at positive surface charges, being replaced by two series of near degenerate reverse $\text{CT}_{\text{Ri}=0-1}$ states at *ca.* 4.50 eV ($\Delta q_{\text{t}} = 0.35/0.55$ a.u.) plus another one with a lesser CT character ($\text{CT}_{\text{R}2}$: 4.75 eV and $\Delta q_{\text{t}} = 0.2/0.25$ a.u.). As expected, CT_{Ri} for the Oin^- anion are much more stable than for neutral Py, but the most remarkable result is the surprising lack of dependence of the respective energies on q_{eff} , *i.e.*, the surface charge does not tune at all the reverse molecule-to-metal electron transfer processes. Therefore, no energy gain $G_{\text{R}} = \text{CS}_{\text{R}} \approx 0$ is predicted given that $S_{\text{R}} \approx 0$.

By carefully observing Fig. 2a a qualitative change in the behaviour of the M–A complex can be realized. Negative or positive surface charge selects one of the two different electronic structures of the M–A complex which have been named as P- or C-hybrids, respectively. This structural change is highlighted in Fig. 2b where the energies of the CT and S_0 states are referred to both fragments M and A at infinite separation ($E_{M\cdots A}$, bond energy). At zero or negative charges ($q_{\text{eff}} \leq 0$) the stability of the system in its ground state ($E_{M\cdots A}$, S_{0-}) varies continuously from +38 to -35 kcal mol $^{-1}$. The largest positive value of +38 kcal mol $^{-1}$ points out to a metastable complex located in a relative minimum where the strong M–A chemical affinity prevents the repulsive dissociation (Fig. S1, ESI†). As in pyridine, these $[(\text{Ag}_n)^q\text{-Oin}^-]^{q-1}$ weakly bonded complexes at $q_{\text{eff}} \leq 0$ can be considered to be a case of physisorption (P-hybrid). In contrast, the bond energies of complexes containing positive silver clusters ($E_{M\cdots A}$, S_{0+}) are less dependent on q_{eff} and much more stable, with typical bond energies of the chemisorbed species (C-hybrid) ranging from -119 to -133 kcal mol $^{-1}$. Therefore, the electronic structure of M–A systems shows very complex dependence on the metal charge which overrides any standard discussion exclusively based on simple coulombic interactions. In the case of adsorbates with negative charge as in $^-$, the electrostatic repulsion between the anion and the metal at negative potentials destabilizes the structure of the surface complex, and the attractive interaction stabilizes it at positive E_{V} . This causes a disruption in the more or less continuous trend shown by the properties of the pyridine–silver system (Fig. 1b). The electronic structure of Ag–Oin $^-$ undergoes a qualitative gap when the surface charge changes its sign ($q_{\text{eff}} \leq 0 \leftrightarrow q_{\text{eff}} > 0$), as shown in Fig. S3 (ESI†), where the main molecular orbitals involved in the CT states are drawn. A quantitative gap of the corresponding energies can be appreciated when q_{eff} is positive/zero or negative which is much less pronounced in the case of pyridine (Fig. S2, ESI†), which allows us to consider the Ag–Py complex as a P-hybrid in the overall range of q_{eff} .

Therefore, the electrode potential is able to select two kinds of surface hybrids for $[(\text{Ag}_n)^q\text{-Oin}^-]^{q-1}$: a P-hybrid characterized by a weak surface complex with properties tunable in a continuous way ($q_{\text{eff}} \leq 0$), and a C-hybrid, a strongly bonded system ($q_{\text{eff}} > 0$) whose electronic structure is hardly modified by E_{V} .

The ground S_0 states of all the discussed M–A complexes show a net donation of negative charge from the adsorbate to the silver cluster ($q_{\text{M} \leftarrow \text{A}, S_0}$), even at negative q_{eff} (Fig. S4a, ESI†). In the case of pyridine, a rather smooth dependence is observed, while for the charged Oin $^-$ a dual behaviour can be seen with

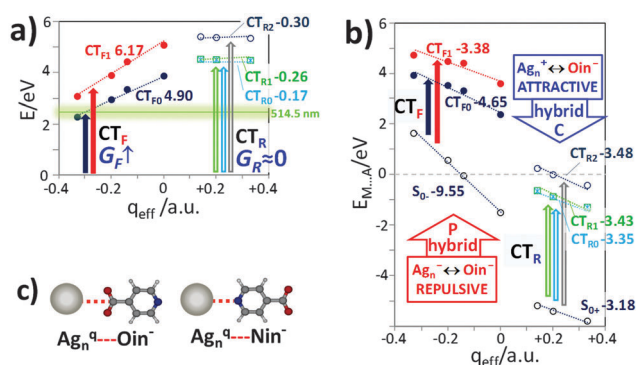


Fig. 2 Dependence on q_{eff} of: (a) TD-M06-HF/LanL2DZ vertical energies (eV) of the forward ($\text{CT}_{\text{Fi}=0,1}$) and reverse ($\text{CT}_{\text{Ri}=0-2}$) charge transfer states of silver–isonicotinate complexes $[(\text{Ag}_n)^q\text{-Oin}^-]^{q-1}$ (each label is accompanied by the slope S (eV a.u. $^{-1}$) in eqn (1)), (b) TD-M06-HF/LanL2DZ energies of the same states but referred to the energy of the metallic clusters (Ag_n^q) and the adsorbate (in^-) at infinite separation ($E_{M\cdots A}$). Arrows correspond to the discussed forward (solid) and reverse (hollow) CT transitions from the ground electronic state S_0 and the colours are arbitrarily assigned. (c) C_{2v} complexes of isonicotinate bonded to silver through the aromatic nitrogen (Ag-Nin^-) or the carboxylate (Ag-Oin^-).

significant slopes at $q_{\text{eff}} \leq 0$, but being almost insensitive at positive charges. In this sense, the S_{0+} ground states of C-hybrids at $q_{\text{eff}} > 0$ already show the CT_R character given that, for instance, Oin^- donates *ca.* -0.35 a.u. to any of the Ag_n^+ clusters. Finally, Fig. S4b (ESI[†]) shows a very good correlation between the strength of the M–A bond ($E_{\text{M} \cdots \text{A}}$) and the charge donated by Py or in^- to the Ag_n cluster in S_0 ($q_{\text{M} \leftarrow \text{A}, S_0}$). Once again both kinds of hybrids are easily recognized.

In order to confirm these results a similar study was carried out on the less stable $[(\text{Ag}_n)^q\text{--Nin}^-]^{q-1}$ complex. The M06-HF results for both complexes as well as those obtained by using the long-range corrected $\omega\text{B97X-D}^{13}$ functional are compared in Tables S1–S3 and Fig. S5 (ESI[†]). All the results predict very similar CT_F states for the P-hybrid. In contrast, the reverse CT_R states of the C-hybrid are dependent on the type of coordination (Ag--Oin^- or Ag--Nin^-) and on the used functional; $\omega\text{B97X-D}$ CT energies *ca.* 2 eV being more stable than the M06-HF ones. However, all the results point out the same conclusions: (i) the existence of two kinds of surface hybrids and (ii) the lack of sensitivity of the energies of any CT_R state to the surface charge, *i.e.* on the electrode potential. A detailed inspection of the CT_{R0} state of Ag--Py also reflects the presence of two different slopes with little dependence on q_{eff} (Fig. 1c).

Summarizing, this communication discusses for the first time the existence of different kinds of hybrid complexes formed by metals bonded to charged molecules corresponding to different electronic structures which are selected by changing the sign of the charge of the metal. Furthermore, the dependence of the forward and reverse CT processes on the surface charge shows an opposite dependence on q_{eff} , predicting either a huge gain or an almost zero efficiency when the electrode potential is used to tune the energy of the respective CT process. This allows for selecting, opening or closing different CT channels acting in opposite electron transport directions. In spite of the fact that this work dealt with small metallic clusters, the results could open new perspectives to a better understanding of the complex behavior of molecules bonded to nanometer or atomic size metallic clusters detected in SERS, single molecule SERS, tip-enhanced Raman scattering (TERS) or in molecular electronics. It must be stressed that our methodology based on standard DFT calculations is able

to predict very surprising behaviours depending on the nature and the respective charges of the metal and the adsorbed molecule. This will allow classification of different types of metal–molecule hybrids in a comprehensive way according to their respective electronic structures.

Finally, the dual electronic structure of M–A suggests a differentiated mechanism for the oxidation and reduction that could play a key role in electrochemistry, adsorption or heterogeneous catalysis, providing alternative explanations to some results discussed so far on, for instance, molecular reorientation.

We are grateful to the Spanish MINECO (CTQ2012-31846) and Junta de Andalucía (FQM-5156/6778) for financial support and to SCAI and Rafael Larrosa (UMA) for computational facilities.

Notes and references

- 1 P. V. Kamat, *Chem. Rev.*, 1993, **93**, 267.
- 2 C. D. Lindstrom and X. Y. Zhu, *Chem. Rev.*, 2006, **106**, 4281.
- 3 L. Cui, D. W. Wu, A. Wang, B. Ren and Z. Q. Tian, *J. Phys. Chem. C*, 2010, **114**, 16588.
- 4 A. Otto, J. Billmann, J. Eickmans, U. Ertürk and C. Pettenkofer, *Surf. Sci.*, 1984, **138**, 319.
- 5 D. M. Kolb, *Angew. Chem., Int. Ed.*, 2001, **40**, 1162.
- 6 J. Roman-Perez, C. Ruano, S. P. Centeno, I. López-Tocón, J. F. Arenas, J. Soto and J. C. Otero, *J. Phys. Chem. C*, 2014, **118**, 2718.
- 7 F. Avila, D. J. Fernández, J. F. Arenas, J. C. Otero and J. Soto, *Chem. Commun.*, 2011, **47**, 4210 and references therein.
- 8 F. Avila, C. Ruano, I. López-Tocón, J. F. Arenas, J. Soto and J. C. Otero, *Chem. Commun.*, 2011, **47**, 4213 and references therein.
- 9 M. J. Frisch, *et al.*, *Gaussian 09, Revision A.02*, Gaussian, Inc., Wallingford CT, 2009.
- 10 Y. Zhao and D. G. Truhlar, *J. Phys. Chem. A*, 2006, **110**, 13126.
- 11 P. J. Hay and W. R. Wadt, *J. Chem. Phys.*, 1985, **82**, 299 and references therein.
- 12 M. R. López-Ramírez, C. Ruano, J. L. Castro, J. F. Arenas, J. Soto and J. C. Otero, *J. Phys. Chem. C*, 2010, **114**, 7666.
- 13 J.-D. Chai and M. Head-Gordon, *Phys. Chem. Chem. Phys.*, 2008, **10**, 6615.